FLOW AND FRACTURE BEHAVIOR OF MOLYBDENUM NEUTRON-IRRADIATED AT 80°C— M. Li, T. S. Byun, N. Hashimoto, L. L. Snead, and S. J. Zinkle (Oak Ridge National Laboratory)

SUMMARY

Low carbon arc cast (LCAC) molybdenum was neutron irradiated at 80°C in the high flux isotope reactor (HFIR) to fluences between 2×10^{21} and 8×10^{24} n/m^2 (E > 0.1 MeV), corresponding to nominal displacement doses of 7.2×10^{-5}, 7.2×10^{-4}, 7.2×10^{-3}, 7.2×10^{-2}, and 0.28 dpa. Tensile tests were performed on unirradiated and irradiated specimens at 100, 22, -25, and -50°C at a strain rate of 1.1×10^{-3} s^{-1}. The fracture surfaces of tensile-tested specimens were examined by scanning electron microscopy. The paper examined the temperature and dose dependence of yield stress, post-yield strain hardening and tensile ductility. The fracture modes of irradiated Mo were also discussed.

PROGRESS AND STATUS

Experimental Procedure

The material examined was low carbon arc cast (LCAC) molybdenum (Ingot No. 50814) provided by Bettis Atomic Power Laboratory. The nominal chemical composition is given in Table 1. Subsize SS-3 tensile specimens were electron-discharge-machined (EDM) from a cold-rolled 0.5 mm thick sheet. The geometry and dimensions of SS-3 tensile specimens are shown in Fig. 1. Following machining specimens were annealed at 1200°C for 1 h in a high vacuum and furnace cooled. The annealed microstructure has equaxied grains with a grain size of 70 µm. Before irradiation SS-3 tensile specimens were mechanically polished with 2400 grit SiC abrasive paper.

Table 1. The nominal chemical composition of LCAC Mo

Mo (%)	Fe (ppm)	Ni (ppm)	Si (ppm)	C (ppm)	O (ppm)	N (ppm)
> 99.95	100	2	100	100	15	20

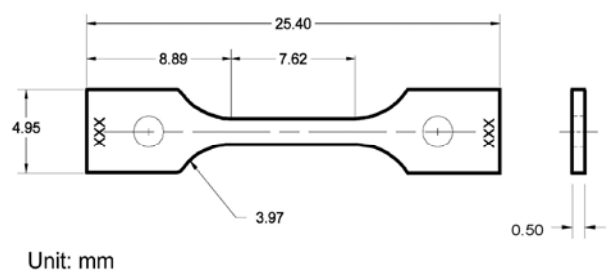

Fig. 1. Dimensions of SS-3 type sheet tensile specimens.

Irradiation of specimens was carried out in the hydraulic tube (HT) facility of the high flux isotope reactor (HFIR) at the ORNL. Four bare SS-3 tensile specimens were loaded in each perforated rabbit capsule allowing contact with the flowing coolant in the hydraulic tube to maintain the specimen temperature at ~ 80°C. Specimens were irradiated to neutron fluences of 2×10^{21}, 2×10^{22}, 2×10^{23}, 2×10^{24}, and 8×10^{24} n/m^2 (E > 0.1 MeV), corresponding to displacement damage levels of 7.2×10^{-5}, 7.2×10^{-4}, 7.2×10^{-3}, 7.2×10^{-2}, and 0.28 dpa. Tensile tests were conducted on unirradiated and irradiated specimens at -50, -25, 22, and 100°C on a screw-driven machine. All tensile tests were performed at a crosshead speed of 0.02 in/min, corresponding to a strain rate of 1.1×10^{-3} s^{-1}. Tensile tests at 20 and 100°C were conducted in air, and -25 and -50°C tests were carried out in a mixed air and cold nitrogen environment. Load and displacement data

were recorded and used to determine stress-strain curves and tensile properties. The engineering stress-strain curves were corrected by the theoretical Young's modulus of molybdenum to eliminate any discrepancy of tests from machine stiffness and specimen loading. The correction of stiffness was made using the following equation:

$$\varepsilon_p = \varepsilon_t - \varepsilon_e = \varepsilon_t - \frac{\sigma}{E_0}$$
$$\varepsilon_t^{corr} = \varepsilon_t - \frac{\sigma}{E_0} + \frac{\sigma}{E} \qquad (1)$$

where ε_p is the plastic strain, ε_t the measured total strain, ε_e the measured elastic strain, ε_t^{corr} the total strain corrected by the Young's modulus, σ the applied stress, E_o the machine stiffness, and E the Young's modulus. The machine stiffness, E_o, was determined from the linear portion of the load-displacement curves. The corrected engineering stress-strain curves were checked by comparing the values of tensile properties such as yield stress, ultimate tensile strength, fracture stress and elongations obtained from the corrected curves and non-corrected curves. After tensile testing, fractographic examinations were performed by scanning electron microscopy (SEM).

RESULTS

Engineering Stress-Strain Curves

Tensile tests were carried out at 22 and 100°C on SS-3 tensile specimens irradiated to 7.2×10^{-5}, 7.2×10^{-4}, 7.2×10^{-3}, 0.072, and 0.28 dpa. Specimens irradiated up to 0.072 dpa were also tested at -25 and -50°C. Duplicated tests were performed on some dose conditions to estimate uncertainty of the data. The engineering stress-strain curves are shown in Fig. 2, and the tensile properties data are summarized in Table 2. The original stress-strain curves were shifted along the strain axis by 5% consecutively for clarity in the figure. It is seen that stress-strain curves have different characteristics at varied irradiation doses and test temperatures. Unirradiated specimens and low dose specimens (7.2×10^{-5}, 7.2×10^{-4} dpa) showed a prominent yield drop and yield elongation followed by significant strain hardening. As doses increased the yield elongation zone gradually disappeared. The flow curves were dominated by an extended plateau with negligent strain hardening after yield drop. As doses increased further, yielding began with a yield drop followed by a continuous load drop to fracture, indicating a lack of homogeneous deformation leading to plastic instability at yield. Some high dose specimens broke in a completely brittle manner at lower temperatures. Test temperatures affect the shapes of stress-strain curves as well. For unirradiated specimens, the yield elongation zone became more evident as temperature decreased. For specimens irradiated to 7.2×10^{-5} dpa, the yield elongation zone showed irregular features at low temperatures. For higher dose specimens, decrease in test temperature led to brittle fracture.

Radiation softening was observed in low dose specimens when tested at 22°C and lower. The yield stress reached a minimum at 7.2×10^{-4} dpa. Irradiation hardening became evident at ~ 0.01 dpa. The hardening effect increased significantly with increasing dose and approached to saturation at ~ 0.1 dpa. The hardening behavior is consistent with the microstructure development during irradiation. The detailed as-irradiated microstructure was described in a previous paper [1]. Similar softening and hardening behavior was observed in Tanaka's experiments [2]. Comparable hardening effect was found in neutron-irradiated mono-crystalline Mo [3], and a smaller hardening effect was observed in proton-irradiated Mo in stress-relieved condition [4]. Byun et al. [5] reported a decrease in the yield strength of powder metallurgy Mo above 0.001 dpa, which is likely due to premature failure caused by grain boundary embrittlement.

Significant hardening was accompanied by severe loss in tensile ductility. Uniform elongation dropped to less than 1% at a dose of 0.072 dpa even at 100°C. The more striking feature is the temperature dependence of embrittling behavior. Specimen failed elastically even at 0.0072 dpa when tested at -50°C.

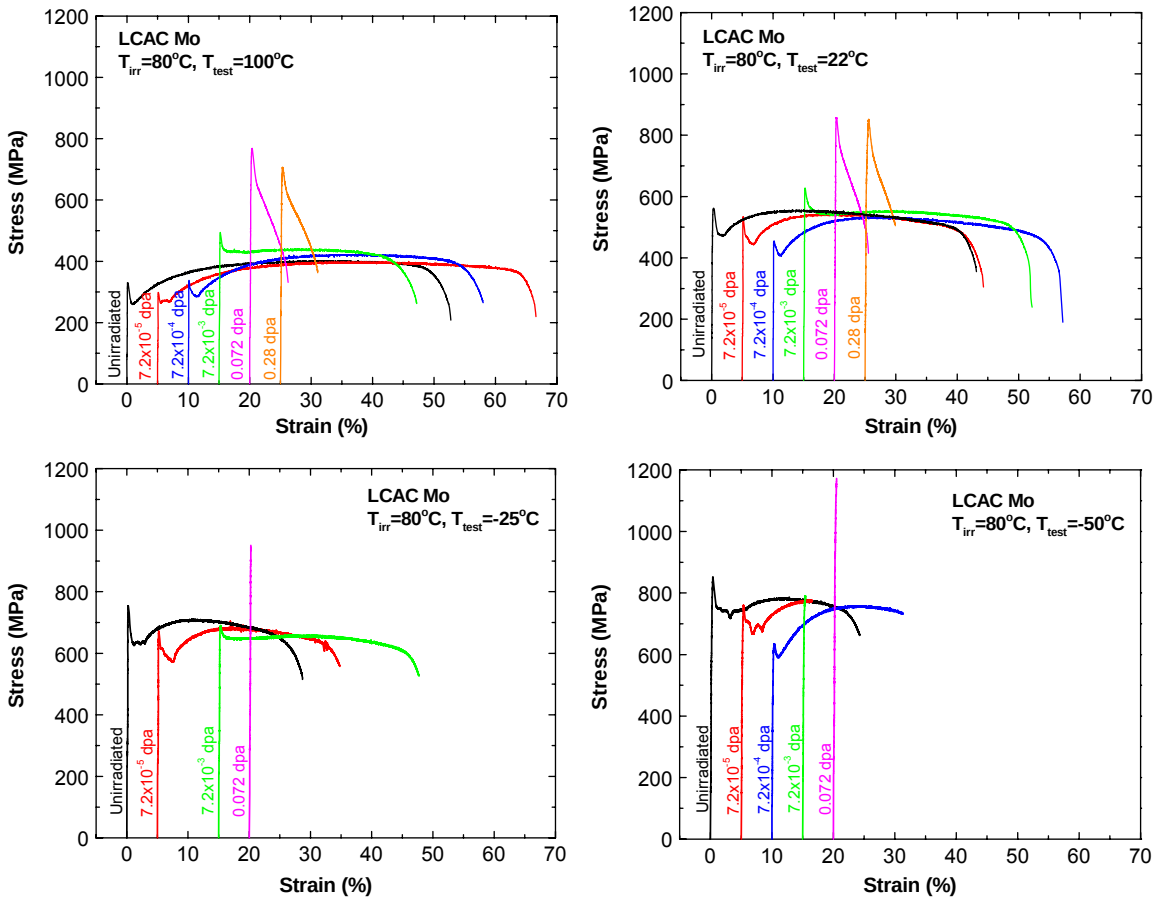

Fig. 2. Engineering stress-strain curves of unirradiated and irradiated LCAC Mo tested between -50 and 100°C.

Table 2. Tensile properties of unirradiated and irradiated LCAC Mo

Test Temp (°C)	Dose (dpa)	UYS (MPa)	LYS (MPa)	UTS (MPa)	UE (%)	TE (%)
22	Unirr	561.8	473.0	552.9	14.6	42.9
	7.2×10^{-5}	531.8	444.6	540.5	15.8	38.9
	7.2×10^{-4}	455.2	409.1	532.9	17.4	46.5
	7.2×10^{-4}	458.2	440.3	562.3	17.2	39.9
	7.2×10^{-3}	627.5	542.6	551.7	13.5	36.5
	7.2×10^{-2}	857.0	748.1	857.0	0.1	5.3
	0.28	796.8	680.3	796.8	0.2	4.9
	0.28	852.6	725.2	852.6	0.3	4.8
100	Unirr	330.8	259.5	402.1	33.2	52.3
	7.2×10^{-5}	298.5	272.4	397.0	31.8	61.3
	7.2×10^{-4}	337.6	291.1	422.0	27.1	47.9
	7.2×10^{-3}	494.5	434.2	440.2	13.0	32.1
	7.2×10^{-2}	768.1	655.6	768.1	0.2	6.2
	0.28	658.7	555.1	658.7	0.1	5.0
	0.28	706.2	621.0	706.2	0.2	6.0
-25	Unirr	694.7	631.6	697.6	11.3	29.2
	Unirr	754.3	633.5	710.1	10.9	28.5
	7.2×10^{-5}	668.9	572.0	680.6	12.8	29.6
	7.2×10^{-3}	690.3	645.5	657.4	13.9	32.6
	7.2×10^{-2}	951.1	951.1	951.1	0.0	0.0
-50	Unirr	849.8	740.4	783.6	11.4	24.1
	7.2×10^{-5}	760.4	669.4	775.1	11.3	11.3
	7.2×10^{-4}	633.8	593.5	757.7	14.2	21.0
	7.2×10^{-3}	790.5	790.5	790.5	0.2	0.2
	7.2×10^{-2}	1172.0	1172.0	1172.0	0.2	0.2

Temperature Dependence of Yield Stress

The yield stress of bcc metals exhibits strong temperature and strain rate dependence at low temperatures. The temperature and strain rate dependence of yielding can be affected by chemical and microstructural changes, and therefore by neutron irradiations. As all the tensile tests were performed at a single strain rate, only the temperature dependence of the yield stress is of interest in this paper. In discussion of temperature dependence of the yield stress, it is necessary to divide the yield stress into two components, an athermal component (practically no temperature dependence) and a thermal component (temperature dependent). Figure 3 shows the yield stress of unirradiated LCAC Mo as a function of test temperature along with the Mo

data from the literature [2,4,6,7]. Note that both annealed and stress-relieved heat treatments are included. The yield stress of Mo increases rapidly with decreasing temperature. The yield stress of annealed Mo apparently reached the athermal regime at 150–200°C (0.15–0.16 T_m), while stress-relieved Mo approached to the athermal regime at about room temperature (0.1 T_m). The difference in yield stress between annealed Mo and stress-relieved Mo is essentially temperature independent, i.e., athermal in nature. The yield stress of LCAC Mo examined in this study is relatively higher than the yield stress of recrystallized Mo studied by Tanaka [2] and by Hasson [7]. This difference is likely associated with material's processing, purity and strain rate. Note that the data reported by Hasson was for single crystal Mo of [110] orientation, and the values of critical resolved shear stress were multiplied by 3.06 so to compare with the yield stress of polycrystalline materials [8].

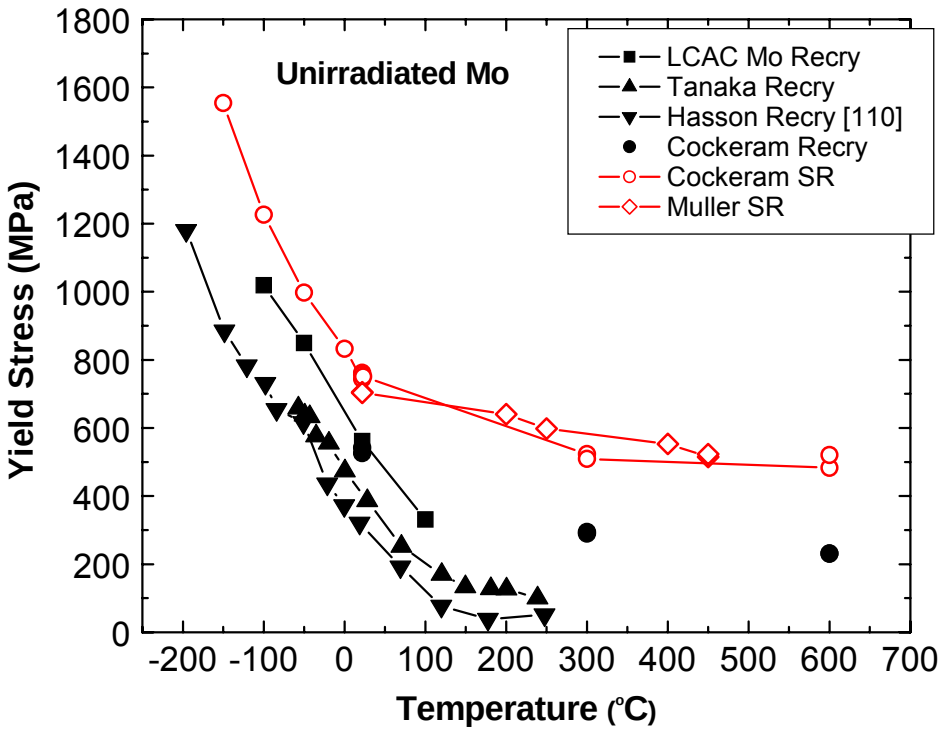

Fig. 3. Temperature dependence of the yield stress of unirradiated Mo.

The temperature-dependent yield stress of irradiated LCAC Mo are shown in Fig. 4 for low dose irradiations (< 0.001 dpa), along with the data reported by Tanaka et al. [2]. In this dose range, the yield stress and its temperature dependence were only slightly affected by irradiations. Reduced temperature dependence was observed both in this study and in Tanaka's work due to radiation-induced softening at low temperatures and hardening at high temperatures. The crossover of radiation softening and radiation hardening is ~ 70°C in the present work and ~ 50°C in Tanaka's experiments. Regarding the dose effect, the radiation softening effect was stronger at 7.2×10^{-4} dpa than at 7.2×10^{-5} dpa with a maximum reduction in yield stress of 16–20%. The decrease in temperature dependence of yielding implies that the irradiation effect was mainly thermal in nature, and the activation energy for thermally-activated dislocation glide was smaller in the irradiated material. There has been significant evidence of radiation-induced softening in bcc metals such as iron, niobium, molybdenum, vanadium, etc. The phenomena of softening caused by defect clusters from irradiation are similar to "alloy softening" in bcc-base alloys that was observed in the low temperature range below 0.15 T_m where obstacles can be overcome by a thermally-activated process [9]. Several models have been proposed to explain the softening effects in bcc metals. The generally-accepted model is the enhanced nucleation of double kinks in the vicinity of small defect clusters. TEM examinations and electrical resistivity measurements

on the specimens irradiated at 7.2×10^{-5} and 7.2×10^{-4} dpa revealed that there was a large population of small glissile defect clusters, and the interactions between these small defect clusters and screw dislocations may be responsible for the observed radiation softening.

The effect of neutron irradiations on the temperature dependence of the yield stress is significantly different at higher doses. Figure 5 shows the yield stress versus test temperature at doses of 0.0072, 0.072, and 0.28 dpa for LCAC Mo. Data reported by Tanaka et al. [2] and Hasson et al. [7] were also presented in Fig. 5 for comparison. Only radiation hardening was observed in the examined dose range, and the increase in yield stress is primarily athermal, which is in contrast to the thermal obstacles at low doses. TEM examinations revealed a high number density of dislocation loops uniformly-distributed in the matrix in the 0.0072 dpa specimen. As doses increased to 0.072 and 0.28 dpa a strong aggregation of dislocation loops occurred, forming rafts. The cluster mean size increased continuously with dose from 1.76 to 3.36 nm between 7.2×10^{-5} and 0.28 dpa with a broader size distribution at high doses. These visible dislocation loops can be effective hardening centers, impeding dislocation motions. When the hardening is superior, it will surpass any softening effects that are caused by small defect clusters or self-interstitial atoms and give an overall athermal hardening at low temperatures. Tanaka et al. estimated the thermal and athermal yield stress in neutron irradiated Mo specimens. His estimation indicated that the thermal component was decreased, while the athermal component increased with increasing doses. The overall effect of irradiation on temperature dependence of yielding is the result of these two combined reactions.

Temperature Dependence of Strain Hardening

Significant increase in yield stress of Mo was accompanied by drastic decrease in uniform elongation after neutron irradiations. The plastic flow was restricted due to loss of strain hardening capacity. The strain hardening behavior of neutron-irradiated Mo was investigated by examining the difference between yield stress (YS) and ultimate tensile strength (UTS). The UTS and YS are plotted in Fig. 6 as a function of test temperature for the unirradiated and irradiated Mo. As test temperature increases, both UTS and YS of unirradiated and irradiated Mo decrease. For the unirradiated Mo, the temperature dependence of ultimate tensile strength is much weaker than that of the yield stress. Moreover, in contrast to the yield stress, the ultimate tensile strength was not effectively altered by neutron irradiations. At lower doses (< 0.01 dpa) when the material has strain hardenability and some degree of uniform deformations irradiation-induced defect clusters evidently changed the temperature dependence of the yield stress but practically had no effects on the ultimate tensile strength. In other word, the yield stress of Mo depends both on test temperature and neutron dose, but the ultimate tensile strength is dependent only on test temperature at a given irradiation temperature. It is also interesting to note that the temperature dependence of the yield stress after low dose irradiations changed towards to the same temperature dependence of the UTS, due to softening effects at lower temperatures. In fact, the yield stress at 7.2×10^{-4} dpa has nearly the same temperature dependence as of the UTS. As doses increased to 7.2×10^{-3} dpa the material showed very limited strain hardening capability, and the temperature-dependent yield stress was very close to the UTS.

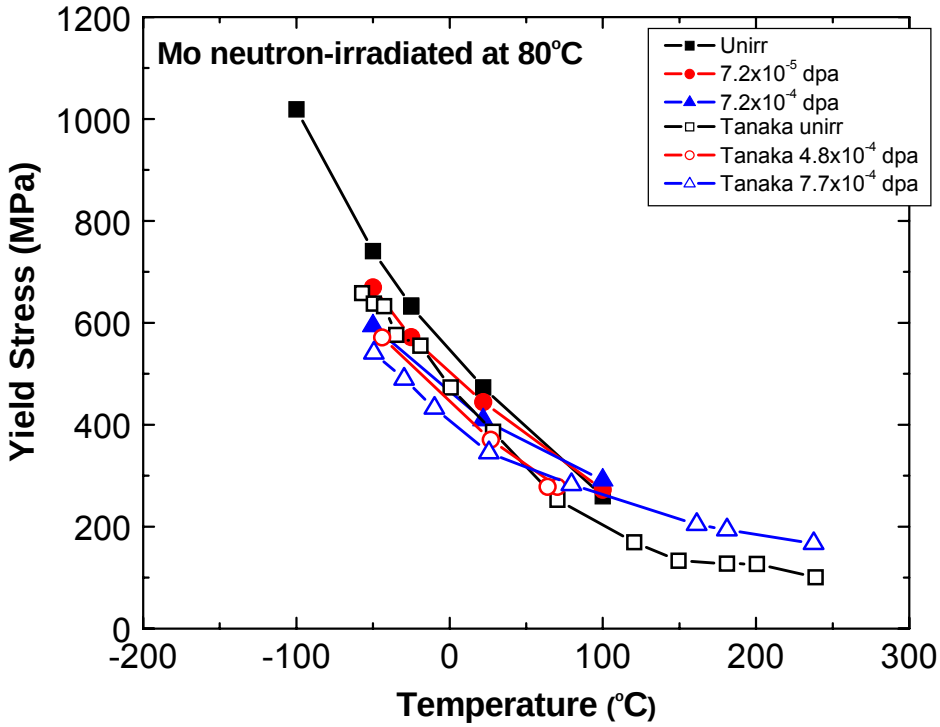

Fig. 4. Radiation effects on temperature dependence of the yield stress of Mo at low doses.

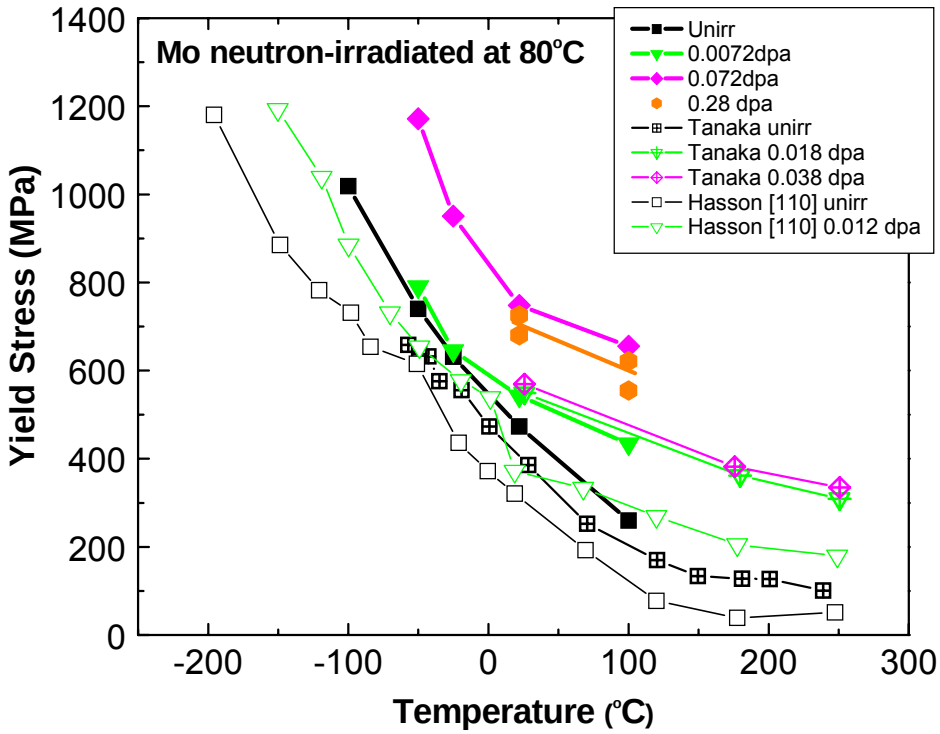

Fig. 5. Radiation effects on temperature dependence of yield stress of Mo at high doses.

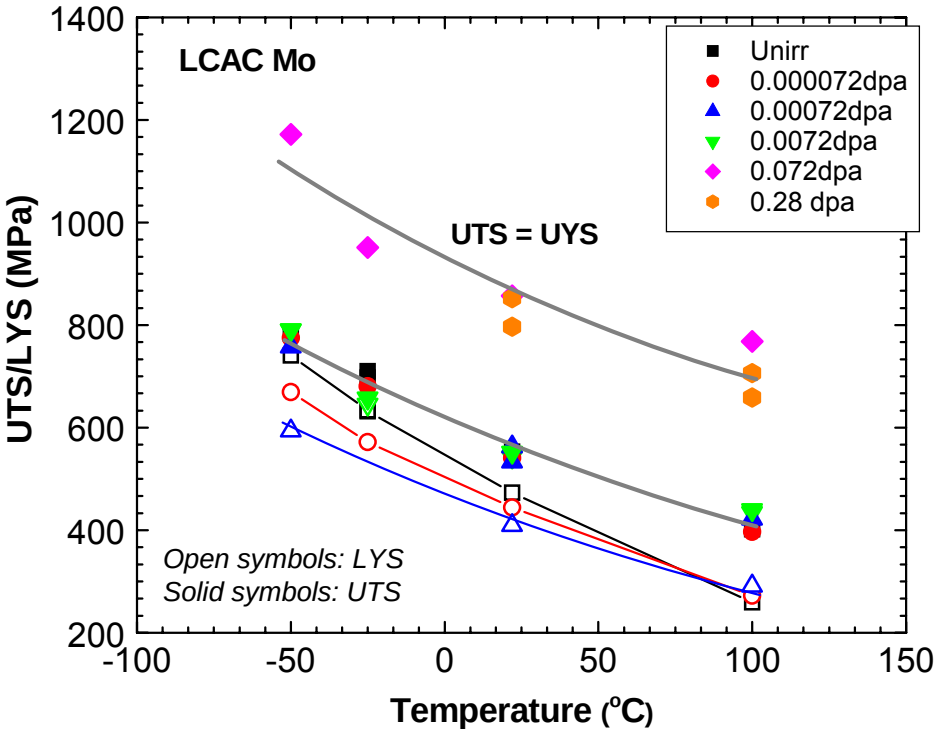

Fig. 6. Temperature dependence of ultimate tensile strength (UTS) of LCAC Mo.

Further irradiations (e.g., 0.072 and 0.28 dpa) caused significant increase in yield stress and complete loss of strain hardenability, leading to severe problems with flow localization and embrittlement. The strength-temperature curves moved upward without changing the temperature dependence, indicating strong athermal hardening. It is suggested that the strain hardening behavior of Mo depends on both doses and test temperature. The dose-independent UTS defines the strength limit where radiation-induced flow localization and embrittlement occurred.

The influence of neutron irradiations on the strain hardening behavior of Mo can be understood further by examining the true stress-true strain behavior. True stress-strain curves were calculated from engineering stress-strain curves up to the point at the onset of necking. The true stress-true strain curves for the unirradiated specimens tested between -50 and 100°C are compared in Fig. 7(a) and their corresponding strain hardening rate-stress curves are shown in Fig. 7(b). It is clear that the yield stress of Mo is very sensitive to temperature in the range of -50 and 100°C, and this difference in yield stress dominates the true stress-true strain curves. The strain hardening behavior shows temperature dependence as well. The strain hardening behavior is comparable at -25 and -50°C with the hardening rate decreasing with flow stress in a nearly linear fashion. At the low stress end around yielding the strain hardening rate decreased rapidly from an initial very high value. As temperature increased to 22°C both high and low stress ends exhibited an upward curvature with an intermittent linear hardening rate similar to low temperature behavior. The initial hardening rate at low stresses was also low relative to -25 and -50°C curves. When tested at 100°C, an extended continuous and gradually-decreasing hardening rate was observed after the linear portion of the curve. The upward tail at the low stress end disappeared at this temperature. For convenience we shall define the rapidly-decreasing low stress end as stage II, the linear portion as stage III and gradually-decreasing high stress end as stage IV.

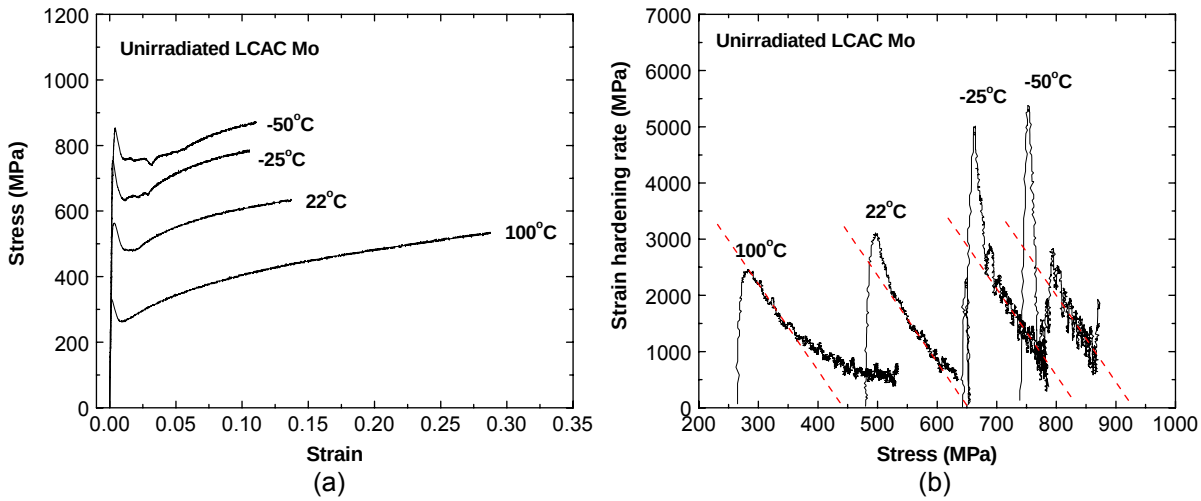

Fig. 7. Unirradiated Mo (a) true stress-true strain curves, (b) strain hardening rate-stress curves.

The true stress-true strain curves and the strain hardening rate–stress curves are shown in Figs. 8 and 9, respectively, for neutron-irradiated Mo. As there is no strain hardenability at any test temperature for specimens irradiated to 0.072 dpa and above, only the strain hardening behavior at 0.0072 dpa and below will be discussed. Note that the end point of strain hardening rate curves is the onset of plastic instability and it is where the hardening rate is equal to the flow stress, i.e., the true stress at necking, $d\sigma / d\varepsilon = \sigma$. The true stress at necking is also defined as the plastic instability stress (PIS) and it is found to be dose-independent parameter for metals and alloys [5,10–12]. It is seen that the plastic instability stress of Mo is independent of neutron irradiation condition but dependent only on test temperature. At 100°C and at doses of 7.2×10^{-5} and 7.2×10^{-4} dpa when slight radiation hardening was observed, the linear hardening behavior (stage III) of irradiated Mo was nearly the same as of unirradiated Mo, and the stage II around yielding varied with doses. As the dose increased to 7.2×10^{-3} dpa when significant radiation hardening occurred, the initial strain hardening rate around yield was very low (~ 800 MPa vs. ~ 3000 MPa for unirradiated Mo), and the hardening rate decreased with decreasing flow stress following the curve of unirradiated Mo and soon reached the PIS. When tested at 22°C, the strain hardening behavior of unirradiated Mo is again similar to unirradiated Mo but the stage II around yield is significantly different between unirradiated and irradiated Mo for low dose irradiations (7.2×10^{-5} and 7.2×10^{-4} dpa). At an intermediate dose (7.2×10^{-3} dpa), the hardening rate is very low, and the hardening rate curve is again overlapped with the curve of unirradiated Mo at high stress end, rapidly reaching the minimum hardening rate. At lower test temperatures, -25 and -50°C, for both unirradiated and irradiated Mo, only stage II and stage III in the hardening rate curves exist. Neutron irradiations at these low doses strongly affected strain hardening within small plastic strain range but had no effect on the dominant linear hardening behavior. In general, at low doses when radiation yield softening and slight hardening occurred, the hardening rate at yield is significantly affected by neutron irradiations. The linear hardening rate behavior is nearly the same for unirradiated and irradiated Mo. At intermediate doses when significant radiation yield hardening occurred and the material still had sufficient uniform elongation, the strain hardening rate was very low, and the hardening rate curve of irradiated Mo was overlapped with the stage III or IV of the unirradiated curve, and soon reached the minimum hardening rate, leading to necking. If the strain hardening rate is plotted as a function of true strain for all the unirradiated and irradiated test conditions, neutron irradiations at low doses (7.2×10^{-5} and 7.2×10^{-4} dpa) have practically no effects on the hardening rate curves except the difference around yielding in a very narrow plastic strain range. Neutron irradiation at an intermediate dose (7.2×10^{-3} dpa) gave almost a constant but very low hardening rate, and the hardening rate increased with decreasing test temperature between 100 and -25°C.

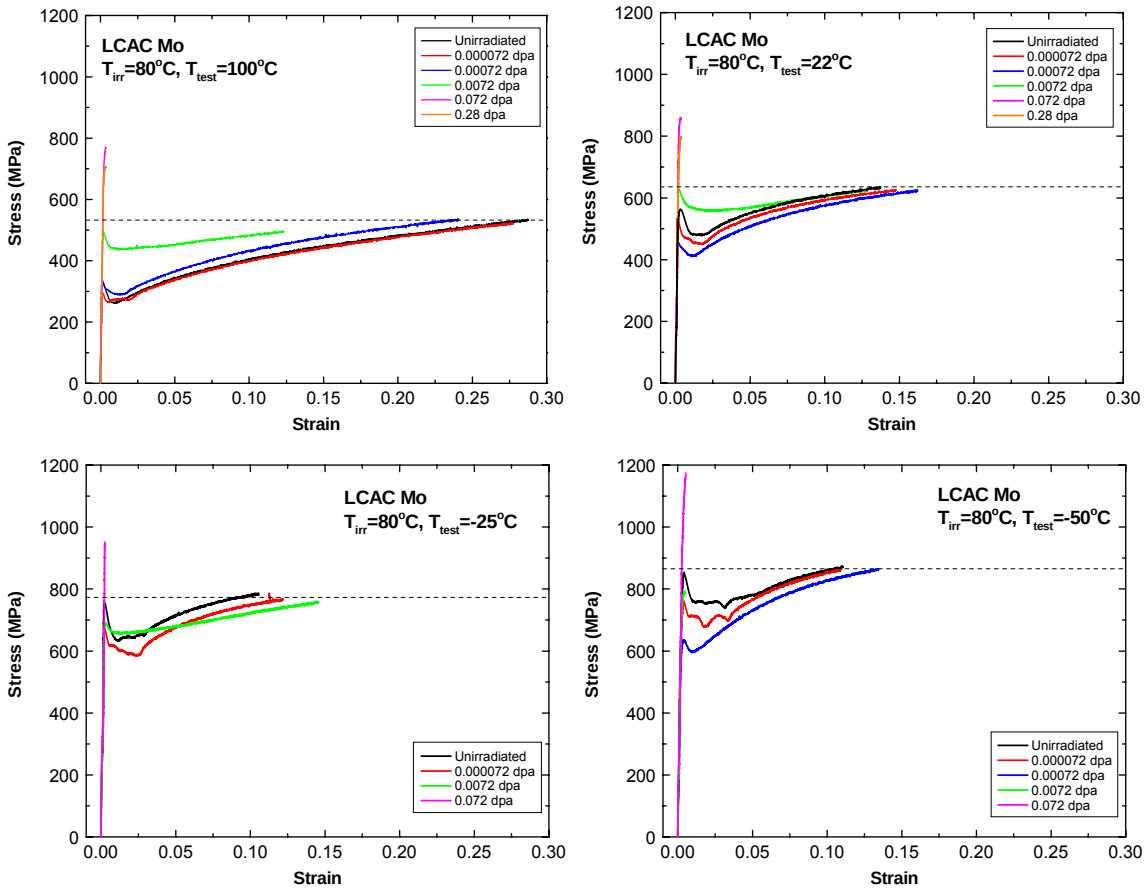

Fig. 8. True stress-true strain curves of unirradiated and irradiated LCAC Mo tested between -50 and 100°C.

The radiation effects on the post-yield strain hardening behavior has been studied widely on fcc metals (e.g., Cu, Ni, Au), model alloys and structural material such as austenitic stainless steels. Previous studies have found that the true stress-true strain curves of irradiated materials were superimposed on the curve of the unirradiated material after shifting the irradiated curves in strain. It was suggested that the strain hardening behavior is dose independent for fcc metals and alloys [11–13]. A remarkable similarity has been found in neutron-irradiated bcc Mo. The irradiated true stress-true strain curves for Mo match very well with the unirradiated curve after shifting the curves in strain to compensate radiation-induced increase or decrease in yield stress. The strain hardening behavior of molybdenum was not changed by irradiation by any means except the initial strain hardening at yielding. This finding is more significant for the Mo neutron irradiated at a moderate dose. The reduced strain hardening at low strains was restored at high strains so that the portion of stress-strain curves at larger strains for the irradiated Mo is superposed on the curve for the unirradiated Mo. This restoration of strain hardenability was suggested to be associated with activation of additional slip systems that assist dislocation network interaction and dislocation multiplication [14]. Strain hardenability capacity appears to be consumed as irradiation dose increases, leading to plastic instability and onset of necking at yield.

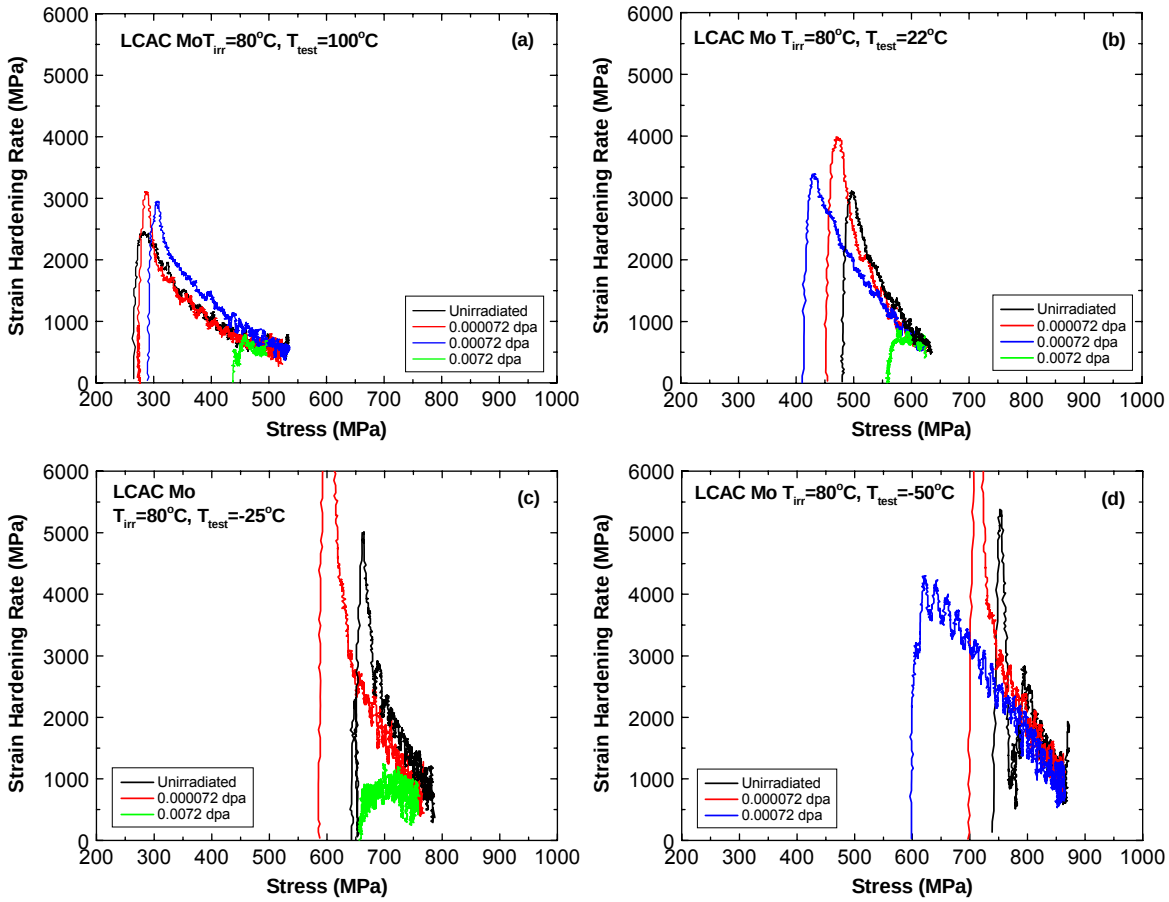

Fig. 9. Strain hardening rate-strain curves of unirradiated and irradiated LCAC Mo tested between -50 and 100°C.

Temperature Dependence of Ductility

Hardening in Mo resulting from low temperature neutron irradiations was accompanied by flow localization and embrittlement, as seen from the stress-strain curves (Fig. 2). Due to strong dose and temperature dependence of yield strength, drastic ductility loss occurred at low temperatures. Figure 10 shows the uniform elongation (UE), total elongation (TE) and reduction in area (RA) as a function of test temperature for LCAC Mo irradiated at five doses. The tensile elongations include the plastic portion only. The reduction in area was determined from low magnification (50×) SEM images of fracture surfaces of the tensile specimens. The projected cross section area at final failure was used to calculate the reduction in area (RA) for the unirradiated and irradiated Mo.

The unirradiated Mo has moderate temperature dependence of tensile ductility. The ductility decreased about 50% as the temperature decreased from 100°C to -50°C but still retained 11% uniform elongation at -50°C. After low dose irradiations (7.2×10^{-5} and 7.2×10^{-4} dpa), tensile ductility changed only slightly. Uniform elongation of irradiated Mo increased relative to unirradiated Mo when radiation softening occurred, and the temperature dependence of uniform elongation was slightly affected. The temperature dependence of ductility was drastically changed after irradiation at 0.0072 dpa. The uniform elongation and total elongation were nearly constant and retained good ductility between -25 and 100°C and then was reduced to < 1%. Interestingly, the reduction in area at 0.0072 dpa was similar to the unirradiated Mo at -25 and 100°C. Evidently irradiations at 0.0072 dpa increased the embrittling temperature of molybdenum. As doses increased

to 0.072 dpa and above, plastic instability occurred at all test temperature due to significant radiation hardening. Total elongation was about 5% at 22 and 100°C but dropped to < 1% below room temperature. The flow localization temperature increased from -50 to 100°C and the embrittling temperature increased from -50 to -25°C as doses increased from 0.0072 to 0.072 dpa. However, the temperature-dependent reduction in area of irradiated Mo was reduced only slightly at 22 and 100°C when the total elongation was strongly affected by irradiation hardening. At -50°C the reduction in area of unirradiated specimens was all below unirradiated specimens.

A strong correlation between the yield stress and uniform elongation has been reported for the irradiated 316SS by Wu et al. [11] and for copper alloys by Pan et al. [12]. To explore the correlation for the irradiated Mo, the yield stress and the plastic instability stress (PIS) are plotted in Fig. 11 in terms of uniform elongation for the unirradiated Mo and irradiated Mo to all doses. At a given test temperature the plastic instability stress of irradiated Mo is constant over the examined dose range. The PIS increased with decreasing test temperature. The PIS defines the stress level where onset of necking takes place at yield and it is solely dependent upon test temperature. Below the plastic instability stress, uniform elongation decreases with increasing yield stress. It is apparent that the reduction in uniform elongation with increasing yield stress is more gradual at a higher test temperature and much more dramatic as test temperature decreased. It is also noted that the minimum observed uniform elongation before flow localization is about 10% at all test temperatures, practically temperature-independent.

Temperature Dependence of Fracture

The fracture surfaces of unirradiated and irradiated specimens tested between -50 and 100°C were examined by scanning electron microscopy. Two major fracture modes were observed for all specimen conditions, i.e., ductile laminate fracture and brittle transgranular cleavage mixed with intergranular brittle fracture. Tensile tests at 100°C result in ductile laminate fracture for the unirradiated and all irradiated specimens. As test temperature decreased to room temperature, the unirradiated Mo failed still in a complete ductile mode, and the irradiated Mo showed different fracture modes depending on the irradiation dose. A transition from layered ductile fracture to transgranular cleavage and intergranular fracture was observed as dose increased. A mixed fracture mode of laminate fracture and transgranular cleavage was observed in the low dose specimens (0.000072 to 0.0072 dpa); at doses of 0.072 and 0.28 dpa transgranular cleavage and brittle intergranular separation became the single dominant fracture mode. Necking is still pronounced in all the specimen conditions at 22 and 100°C. When tested at lower temperatures, -25 and -50°C, nearly all the unirradiated and irradiated specimens showed complete transgranular cleavage and intergranular fracture. Necking was observed in the unirradiated and 0.000072 and 0.0072 dpa specimens tested at -25°C and in the unirradiated and 0.00072 dpa specimens tested at -50°C, but the reduction in area is significantly lower compared to those of 22 and 100°C specimens. No necking occurred in the 0.000072, 0.0072, and 0.072 dpa specimens at -50°C. In general the fracture mode of irradiated Mo depends both on irradiation dose and test temperature. Increase in test temperature and decrease in dose changed the mode of fracture from brittle to ductile.

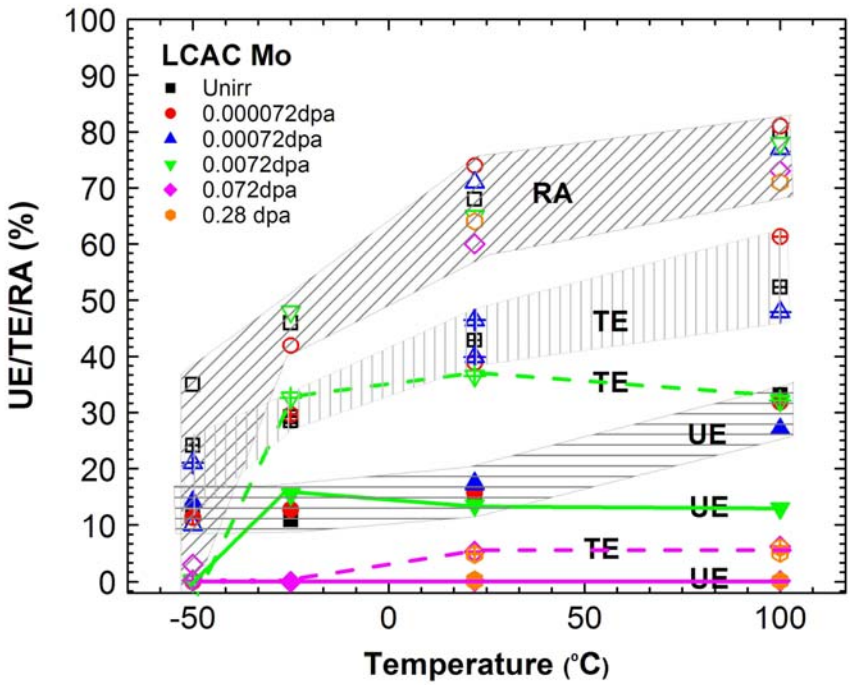

Fig. 10. Temperature dependence of uniform elongation (UE), total elongation (TE), and reduction in area (RA) of neutron-irradiated Mo.

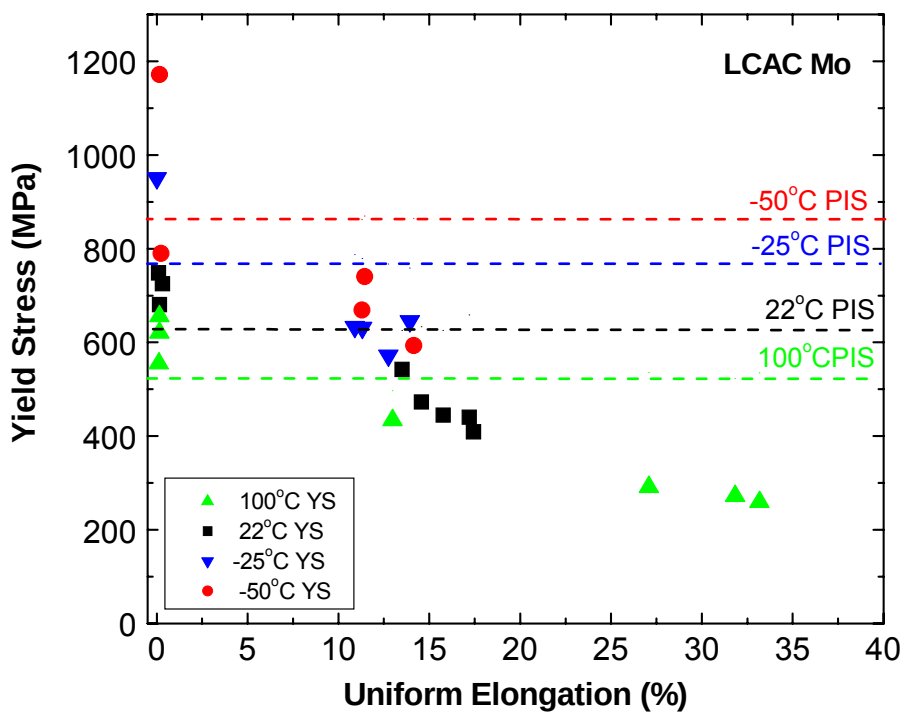

Fig. 11. The correlation between yield stress and uniform elongation of irradiated Mo.

Layered ductile fracture is commonly observed in neutron irradiated Mo [6,15]. Layered structure consists of a stack of thin deformed layers, and it may be associated with the maintained texture by cold rolling after annealing treatment. Grain boundary cracking is the major brittle fracture mode observed in neutron-irradiated, and it has been assumed to be associated with either grain boundary embrittlement by segregated impurity atoms [16] or grain boundary sliding and separation due to irradiation-induced hardening in the grain interior [17]. In the present work, brittle transgranular cleavage was the dominant fracture mode leading to severe reduction in ductility. Singh et al. [3] studied mono- and polycrystalline molybdenum and Mo-Re in order to clarify whether grain boundaries play an important role in irradiation-induced reduction in ductility, and they found that mono- and polycrystalline Mo and Mo-Re deformed in almost the same way after neutron irradiation. Singh et al. suggested that cracks may nucleate at internal or external flaws in the material and propagate without plasticity when the material is significantly hardened. Both their results and the evidence given in this study ruled out grain boundary segregation.

The fracture stress was calculated by the recorded fracture load divided by the cross-section area measured by SEM after failure, and the fracture stress and plastic instability stress are plotted as a function of test temperature in Fig. 12. It needs to be pointed out that the cross-section area determined from SEM images is the projected area. There were no corrections on angular distribution and surface roughness of the cross-section. There was no correction on triaxiality of stress state for the fracture stress calculation either. Fracture modes are also indicated for each irradiation and test condition. Transgranular cleavage fracture was categorized as types I, II, and III according to Gandhi and Ashby [18]. Cleavage I refers to a totally brittle cleavage failure from a pre-existing flaw when the stress is well below the general yield; cleavage II refers to an almost brittle fracture from a plasticity-nucleated crack below the general yield; cleavage III a brittle failure above general yield with measurable fracture strain. Both cleavage II and III fracture were observed in neutron-irradiated Mo. At 22 and 100°C when specimens failed either in a ductile mode or a cleavage mode with evident plasticity the fracture stresses are higher than the PIS, and no evident dose dependence of fracture stress is seen in the figures. Within scatter of data, the fracture stress is apparently constant between 22 and 100°C, as shown in the shaded band in Fig. 12. As test temperature decreased to -25°C, no ductile fracture was observed and the fracture stresses for both unirradiated and irradiated Mo are lower than the constant fracture stress at higher temperature. The fracture stresses at -50°C showed a large scatter of data. The fracture stress of 0.072 dpa specimen is essentially equal to the constant fracture stress at 22 and 100°C, while the unirradiated Mo showed a 200 MPa smaller fracture stress, nearly the same as the fracture stress at -25°C, and the specimens irradiated between 0.000072 and 0.0072 dpa had a fracture stress equal to the PIS at low doses. Recall that the reduction in area at -50°C for unirradiated and irradiated Mo also showed a large scatter of data. With the very high stress, very low ductility, large scatter of reduction in area, it is suggested that the fracture stress at -50°C is close to cleavage stress. What is not understood is if neutron irradiations really have any effects on fracture stresses for cleavage. It appears that the PIS is a more appropriate parameter than the fracture stress that describes the fracture mode at a given dose and test temperature. Neutron irradiations at high doses when plastic instability at yield or embrittlement occurred, the boundaries between fracture fields were shifted.

Acknowledgements

The research was sponsored by the Office of Fusion Energy Sciences, the U.S. DOE under contract DE-AC05-00OR22725 with ORNL, managed and operated by UT-Battelle, LLC. The material was provided by Brian Cockeram at Bettis Atomic Power Laboratory. The authors would like to thank J. L. Bailey, A. M. Williams, L. T. Gibson, and P. S. Tedder for their technical support.

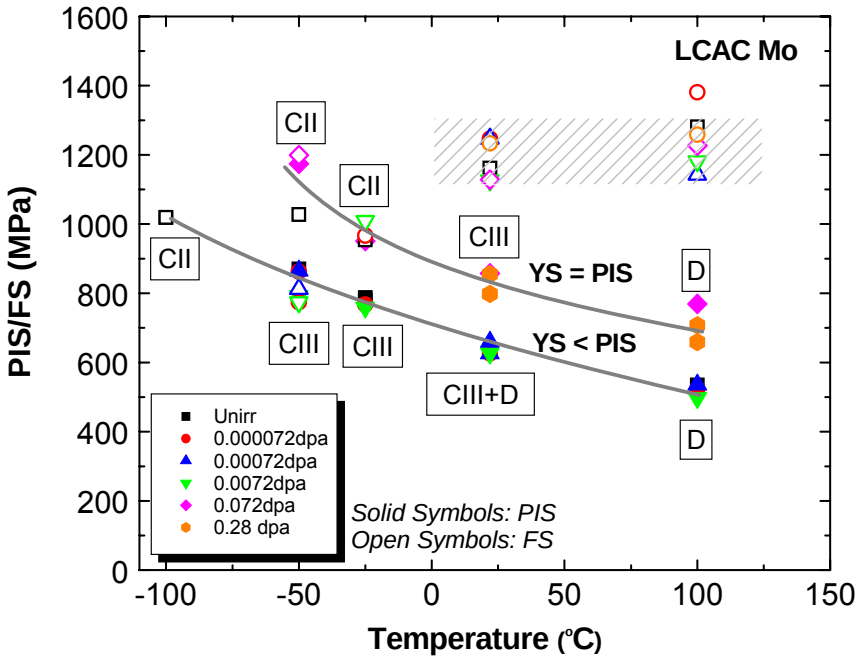

Fig. 12. Temperature dependence of plastic instability stress (PIS) and fracture stress (FS). Fracture modes are also indicated with CIII representing cleavage III, CII cleavage II, and D ductile fracture.

References

[1] M. Li, N. Hashimoto, T. S. Byun, L. L. Snead, and S. J. Zinkle, Journal of Nuclear Materials (ICFRM12).
[2] M. Tanaka, K. Fukaya, and K. Shiraishi, Tran JIM 20 (1979) 697.
[3] B. N. Singh, J. H. Evans, A. Horsewell, P. Toft, and G. V. Műller, J. Nucl. Mater. 258–263 (1998) 865.
[4] G. Műller, Ph.D. thesis, Ėcole Polytechnique Fėdėrale de Lausanne, 1997.
[5] T. S. Byun, K. Farrell, and N. Hashimoto, J. Nucl. Mater. 329–333 (2004) 998.
[6] B. V. Cockeram, J. L. Hollenbeck, and L. L. Snead, J. Nucl. Mater. 324 (2004) 77.
[7] D. F. Hasson, Y. Huang, E. Pink, and R. J. Arsenault, Metall. Trans. 5 (1974) 371.
[8] R. E. Stoller and S. J. Zinkle, J. Nucl. Mater. 283–287 (2000) 349.
[9] E. Pink and R. J. Arsenault, Low temperature softening in body-centered cubic alloys, Prog. Mater. Sci. 24 (1979).
[10] T. S. Byun and K. Farrell, Acta Mater. 52 (2004) 1597.
[11] X. Wu, X. Pan, M. Li, and J. F. Stubbins, J. Nucl. Mater. 343 (2005) 302.
[12] X. Pan, X. Wu, M. Li, and J. F. Stubbins, J. Nucl. Mater. 329–333 (2004) 1088.
[13] R. J. DiMelfi, D. E. Alexander, and L. E. Rehn, J. Nucl. Mater. 252 (1998) 171–177.
[14] S. J. Zinkle and Y. Matsukawa, J. Nucl. Mater. 329–333 (2004) 88.
[15] A. Hasegawa and K. Abe et al., J. Nucl. Mater. 233–237 (1996) 565.
[16] I. V. Gorynin et al., J. Nucl. Mater. 191–194(1992) 421.
[17] B. N. Singh et al., J. Nucl. Mater. 223 (1995) 95.
[18] C. Gandhi and M. F. Ashby, Acta Metall. 27 (1979) 1565.